

## THE GAS CONSUMPTION HISTORY TO $Z \sim 4$

AMBER BAUERMEISTER, LEO BLITZ AND CHUNG-PEI MA  
Department of Astronomy, University of California at Berkeley,  
601 Campbell Hall MC 3411, CA 94720  
SUBMITTED TO APJ: *September 18, 2009*

### ABSTRACT

Using the observations of the star formation rate and H I densities to  $z \sim 4$ , with measurements of the Molecular Gas Depletion Rate (MGDR) and local density of H<sub>2</sub> at  $z = 0$ , we derive the history of the gas consumption by star formation to  $z \sim 4$ . We find that closed-box models in which H<sub>2</sub> is not replenished by H I require improbably large increases in  $\rho(H_2)$  and a decrease in the MGDR with lookback time that is inconsistent with observations. Allowing the H<sub>2</sub> used in star formation to be replenished by H I yields approximately the same solutions as the closed box model since observations show that there is very little evolution of  $\rho_{HI}(z)$  from  $z = 0$  to  $z = 4$ . We show that to be consistent with observational constraints, star formation on cosmic timescales must be fueled by intergalactic ionized gas, which may come from either accretion of gas through cold, but ionized, flows or from ionized gas associated with accretion of dark matter halos. We derive a lower limit to the rate at which the extragalactic ionized gas must be converted into H I and ultimately into H<sub>2</sub> to be about  $1 - 2 \times 10^8 M_{\odot} \text{ Gyr}^{-1} \text{ Mpc}^{-3}$  from  $z \simeq 1 - 4$ . Between  $z = 1$  and  $z = 0$  this mass flow rate decreases by about an order of magnitude with details depending largely on MGDR(t). All models considered require the volume averaged density of  $\rho_{H_2}$  to increase by a factor of 1.5 - 10 to  $z \sim 1.5$  over the currently measured value. Because the molecular gas must reside in galaxies, it implies that galaxies at high  $z$  must be, on average, more molecule rich than they are at the present epoch.

*Subject headings:* Galaxies:ISM — Galaxies:evolution — Stars:Formation

### 1. INTRODUCTION

The time variation of the mean star formation rate in galaxies is by now well established (Madau et al. 1996; Steidel et al. 1999; Hippelein et al. 2003; Hopkins & Beacom 2006), but little is known as to why it takes the functional form it does. The star formation rate is either flat or slowly rising with time, reaching a maximum near  $z \sim 1 - 2$ , and then declines precipitously down to the current epoch. This change in the star formation rate must be closely coupled to both the inventory of gas available for star formation, and the way in which this gas is channeled into galaxies.

Stars condense only from molecular gas at the current epoch and at all epochs in the past. This statement derives from both observational and theoretical considerations. Observationally, the youngest stars are always found to be associated with their nascent molecular material both in the local Universe and at high  $z$  (e.g. Blaauw (1964); Herbig & Kameswara Rao (1972); Schwartz et al. (1973); Omont et al. (1996); Carilli et al. (2002)). The interstellar gas in star forming regions is almost completely molecular, representing a stable phase of the ISM with little atomic content (Burton et al. 1978). Theoretically, there is general consensus that the initiation of star formation requires the nascent gas to become Jeans unstable, probably mediated by magnetic fields (Shu et al. 1987). In star forming regions,  $T$  is typically 10 - 20 K, but in any event cannot be less than 2.7 K. In order to get a solar mass star at 10 K, the Jeans instability criterion would require a density of  $\rho_J > (kT/\mu m_H G)^3 (\pi^5/36M_{\odot}^2) \sim 10^6 \text{ cm}^{-3}$  if a molecular core forms a star at 100% efficiency. The density

must be higher if the efficiency is lower as many observations now suggest (e.g. Motte et al. (1998); Alves et al. (2007); Myers (2008)). In order to reach these temperatures and densities, the gas must be fully molecular to be able to achieve the necessary cooling. We would therefore expect that, in a broad sense, the gas consumption rate is closely tied to the star formation rate.

Unfortunately, there are few constraints on the gas from observations because little is known about the distribution of neutral gas at high  $z$ . There are very few detections of atomic gas in emission at  $z \gtrsim 0.1$ , and what little we know about the atomic gas comes from Lyman-alpha lines seen in absorption toward quasars and radio-loud AGN (e.g. Prochaska & Wolfe 2009; Wolfe et al. 2005; Zwaan & Prochaska 2006). Molecular line observations at high- $z$  have been largely limited to the brightest objects, though some recent observations at  $z \sim 2$  have begun to probe lower luminosity systems (Forster Schreiber et al. 2009; Tacconi et al. 2009).

In this paper, we look at the issue in reverse. Using observations at  $z = 0$ , we examine which quantitative conclusions can be extrapolated to high  $z$ , and using observations of the star formation history, we make several inferences about how the gas consumption into stars must have proceeded. We find that the relationship of the inventory of gas to that of the stars is not straightforward: the observations imply that that all phases of the interstellar and intergalactic medium must be taken into account in order to understand how the gas forms stars. Building a model that includes all the gas phases, we make predictions about gas densities and their variation at intermediate- and high- $z$ , and how this gas must have been accreted into galaxies.

The paper is organized as follows. §2 describes the

observations of the SFRD, MGDR,  $\rho_{H_2}$  and  $\rho_{HI}$  that we use as inputs to our models. In §3, we build three models to fit the observations: the restricted closed box model, the general closed box model and the open box model. In §4, we discuss potential changes to our star formation prescription at high redshift and examine the predictions of the open box model. Appendix A gives the functional form of the smoothed star formation rate density curves we use as an input to our models. Throughout this paper, we adopt a standard  $\Lambda$ CDM cosmology with  $(h, \Omega_M, \Omega_\Lambda) = (0.7, 0.3, 0.7)$ . All of the densities are in comoving units.

## 2. OBSERVATIONS

### 2.1. SFRD

The observed (comoving) star formation rate density, SFRD, was estimated by Madau et al. (1996) over a large range of  $z$  and re-examined by several other investigators (Steidel et al. 1999; Hippelein et al. 2003; Hopkins & Beacom 2006). We will focus on the results of Hopkins & Beacom (2006), a compilation of SFRD measurements at different wavelengths. The measurements are converted to a common cosmology, SFRD calibration, and dust obscuration correction; the data are then fit to a piecewise linear form in  $\log(1+z)$  vs.  $\log(SFRD)$  space as well as the parameterization from Cole et al. (2001). Hopkins & Beacom (2006) find that changing the assumed IMF corresponds to a simple change in the overall amplitude of the SFRD, so each fit is done using two extreme IMF forms in order to provide bounds on the actual form. These two extreme forms for the IMF are a modified Salpeter A IMF and the form of Baldry & Glazebrook (2003). Fig. 1 shows our smoothed form of the Hopkins & Beacom (2006) piecewise linear fit (solid) as well as the Hopkins & Beacom (2006) fit to the Cole et al. (2001) parameterization (dashed) for the two extreme IMFs. Our smoothed piecewise linear forms deviate from the piecewise linear fits of Hopkins & Beacom (2006) only near  $z \sim 1$ . The form of the smoothed piecewise linear fit is given in Appendix A.

At  $z = 0$ , the SFRD fits from Hopkins & Beacom (2006) predict a local SFRD of  $(0.8 - 1.5) \times 10^{-2} M_\odot \text{Mpc}^{-3} \text{yr}^{-1}$ . In an extensive study of galaxies in the local universe (to  $z = 0.1$ ), Salim et al. (2007) find that the SFRD is  $1.828^{+0.148}_{-0.039} \times 10^{-2} h_{70} M_\odot \text{Mpc}^{-3} \text{yr}^{-1}$  from UV observations, a value they argue is the most accurate determination of this number to date. This value (shown as a data point in Fig. 1) is indeed close to those found from other recent investigations (Houck et al. 2007; Hanish et al. 2006) and is also in reasonable agreement with the forms of Hopkins & Beacom (2006).

The agreement between the locally determined SFRD and extrapolation from studies at higher  $z$  (Hopkins & Beacom 2006; Steidel et al. 1999; Hippelein et al. 2003) is encouraging and provides some confidence that the star formation rates and their time variation are being measured reliably. While somewhat different functional forms for the decline of the SFRD with time have been proposed in the literature, e.g.,  $\log(SFRD)$  has been found to be linear in  $z$  (Steidel et al. 1999), in  $t$  (Hippelein et al. 2003), and in  $\log(1+z)$  (Hopkins & Beacom 2006), these

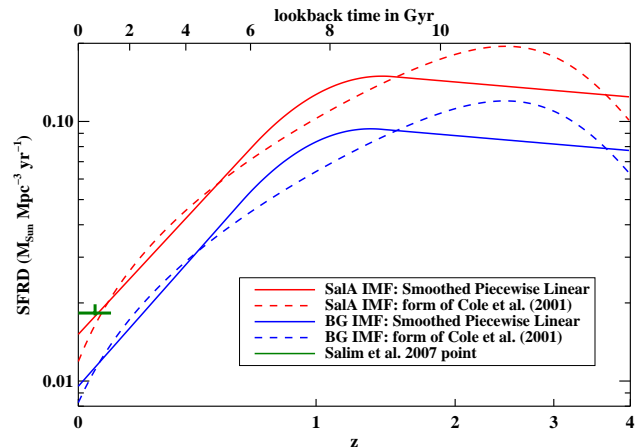


FIG. 1.— Forms of the SFRD. The red curves use the modified Salpeter A IMF (Sala IMF) and the blue curves use the IMF from Baldry & Glazebrook (2003) (BG IMF). The solid red and blue lines show our smoothed version of the piecewise linear fits from Hopkins & Beacom (2006). The fits to the Cole et al. (2001) form are dashed. The SFRD at  $z = 0$  measured by Salim et al. (2007) is in green.

differences have only a small quantitative effect in what follows.

### 2.2. MGDR

#### 2.2.1. Measurements at $z = 0$

The star formation efficiency, SFE, is often defined as the star formation rate per comoving volume divided by the mass per comoving volume of gas; its units are  $\text{yr}^{-1}$  (e.g. Leroy et al. (2008) and references therein). Defined in this way, the SFE is not properly an efficiency, but a rate, and we drop this unfortunate usage even though it has become firmly entrenched in the observational literature. Since we are interested in  $SFE_M$ , the star formation rate density divided by the density of molecular gas,  $\rho_{H_2}$ , we introduce the molecular gas depletion rate, MGDR, to replace the usage of  $SFE_M$ . We define MGDR as SFRD divided by the density of molecular hydrogen,  $\rho_{H_2}$  (this does not include He). The inverse of MGDR is the molecular gas depletion time,  $\tau_M$ , which represents the time it takes to consume all of the molecular gas at the current rate of star formation.

Recently, Leroy et al. (2008) have measured MGDR ( $z = 0$ ) from a comprehensive analysis of 23 nearby galaxies using the THINGS H I survey (Walter et al. 2008) to measure H I surface densities, the BIMA SONG (Helfer et al. 2003) and HERACLES (Leroy et al. 2008b) CO surveys to infer  $H_2$  surface densities, and both SINGS (Kennicutt et al. 2003) and GALEX (Gil de Paz et al. 2007) data to measure star formation rates. The galaxies surveyed include spiral and dwarf galaxies and the analysis was done on a pixel-by-pixel basis convolved to a common resolution, typically  $\sim 800$  pc. This comparison is the most extensive work done to date and the authors find a remarkable constancy of MGDR over a wide range of conditions:  $5.25 \pm 2.5 \times 10^{-10} \text{yr}^{-1}$ , equivalent to a molecular gas depletion time of  $1.9 \times 10^9$  yr. Their measured star formation rates and  $H_2$  column densities vary by three orders of magnitude averaged over entire galaxies, and the pixel-by-pixel values vary even more. Thus the constancy of the MGDR occurs over a wide range

of conditions both within galaxies (including nuclei and disks) and from galaxy-to-galaxy.

### 2.2.2. Measurements at high $z$

The Leroy et al. (2008) study only applies to galaxies near  $z = 0$ . To extend the range of  $z$  we appeal to observations of the MGDR in  $z \gtrsim 1$  galaxies. Daddi et al. (2008) find  $\tau_M/X_{CO} \sim 0.2 - 0.3$  Gyr for two BzK galaxies at  $z \sim 1.5$  ( $X_{CO}$  in  $M_\odot pc^{-2} (K km s^{-1})^{-1}$ ). The  $\tau_M$  they quote however is total molecular gas, including He, so we divide by 1.4 to find the  $\tau_M$  we have defined which does not include He. Therefore, this range corresponds to an MGDR of  $\sim 4.7 - 7$  Gyr $^{-1}$  for a typical ULIRG value of  $X_{CO} \sim 1$  or MGDR = 1 - 1.5 Gyr $^{-1}$  for a Milky Way-like value of  $X_{CO} \sim 4.6$ , about twice the Leroy et al. (2008) value for  $z = 0$ . Similarly, Tacconi et al. (2009) have made an extensive survey of BzK, BX/BM, and submm galaxies at redshifts of 1 and 2, measuring the MGDR for a sample of 26 galaxies. The Tacconi et al. (2009) results use a Milky Way-like value for  $X_{CO}$ .

While the submm galaxies are thought to be responsible for only about 10% of the star formation at these redshifts, Reddy et al. (2005) find that the BzK galaxies (and similar BX/BM galaxies) account for an SFRD of  $\sim 0.1 M_\odot Mpc^{-3} yr^{-1}$  in the range  $1.4 < z < 2.6$ . This is most of the observed SFRD (see Fig. 1), implying that these galaxies dominate the SFRD in this redshift range. The MGDR value that typifies these galaxies should therefore describe the average cosmic MGDR that we use in Eq. 1 for  $z \sim 2$ . This motivates us to use the observations from Daddi et al. (2008) and the 16 BzK and BX/BM galaxies from Tacconi et al. (2009) to constrain our guessed forms of MGDR at other redshifts.

Numerous other authors have estimated the MGDR from individual high redshift galaxies, or from starbursts of ULIRGS (e.g. Gao & Solomon (2004)), and all have found that the MGDR is greater in these galaxies than is typical of galaxies at  $z = 0$ . In fact, there is no observational evidence for a declining MGDR with increasing redshift to at least  $z \sim 4$ . Taken together, all of these observations lead us to reject any model of gas consumption that *requires* lower MGDR values at redshifts significantly greater than zero.

### 2.3. $\rho_{H_2}$

Using a combination of CO and H I measurements in the local universe, Obreschkow & Rawlings (2009) have determined the density of  $H_2$  at  $z = 0$ ,  $\rho_{H_2}(0)$ , to be  $1.9 - 2.8 \times 10^7 \pm 40\%$   $h M_\odot Mpc^{-3}$ . The range of values corresponds to different assumptions about how metallicity affects the CO-to- $H_2$  conversion ratio. Using  $h = 0.7$  gives  $\rho_{H_2}(0) = (1.3 - 2.0) \times 10^7 \pm 40\%$   $M_\odot Mpc^{-3}$ , or an average value of  $1.65 \times 10^7 M_\odot Mpc^{-3}$ . This value is within 50% of the estimate of  $\rho_{H_2}(0) = 1.1 \times 10^7 M_\odot Mpc^{-3}$  by (Zwaan & Prochaska 2006) using a different set of observations and should therefore be reasonably reliable.

### 2.4. $\rho_{HI}$

A number of recent studies have reported measurements of the mean H I comoving mass density in galaxies,  $\rho_{HI}(z)$ , from the local universe to  $z \sim 6$ . At  $z = 0$ , Zwaan et al. (2005) present a study of the H I mass function using the H I Parkes All Sky Survey (HIPASS) data.

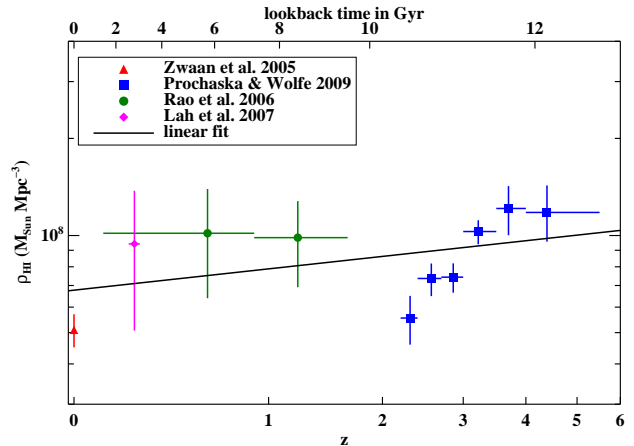


FIG. 2.— Data points for the comoving  $\rho_{HI}$  from Zwaan et al. (2005); Rao et al. (2006); Lah et al. (2007); and Prochaska & Wolfe (2009) with linear fit in  $\log(1+z)$  vs  $\log(\rho_{HI})$  space.

At low redshift, Lah et al. (2007) calculate  $\rho_{HI}$  by co-adding H I 21-cm emission from galaxies with known positions and redshifts. At higher redshifts, estimates of  $\rho_{HI}$  are mainly obtained from DLA studies (Rao et al. 2006; Prochaska & Wolfe 2009). We use these observations of H I to construct an analytical form for  $\rho_{HI}$  as a function of  $z$ . We fit a straight line to these points in  $\log(1+z)$  vs  $\log(\rho_{HI})$  space. The data points and the fit are shown in Fig. 2. The observations suggest very little evolution of  $\rho_{HI}$ , which increases by only a factor of 2-3 between  $z = 0$  and  $z = 6$ .

### 3. BUILDING A MODEL TO FIT THE OBSERVATIONS

The observations above allow us to compare the evolution of the SFRD and  $d\rho_{H_2}/dt$ . We start with the simplest model possible: a closed box of  $H_2$  being turned into stars at the rate of  $d\rho_{H_2}/dt$ . In this simple closed box model, we initially assume that the MGDR is constant in time (the restricted closed box model; §3.1) and subsequently relax this condition (the general closed box model; §3.2). The failure of both models motivates us to consider an open box model (§3.3), where we allow the densities of all four phases of the IGM – stars,  $H_2$ , H I and H II – to vary to match the observational constraints.

We assume that the molecular gas is depleted only through star formation, and that any  $H_2$  dissociated or ionized by star formation is instantaneously returned to the molecular state. Given the short timescales for the formation of molecular gas from its atomic form,  $\sim 10^6$  yr at the relevant densities (Hollenbach & Salpeter 1971; Cazaux & Tielens 2004), this approximation should be a very good one for the purposes of this paper. In any event, if we define  $d\rho_{H_2}/dt$  to be the *net* flow rate of molecular gas into stars, then there is no ambiguity.

We write the statement that star formation occurs only through the depletion of molecular gas:

$$SFRD = MGDR \times \rho_{H_2} \quad (1)$$

This equation is motivated by the constancy of the MGDR at  $z = 0$  (Leroy et al. (2008), see §2.2). We use this prescription for the SFRD for our models but we note that the form may change at higher redshift (See §4.1).

We use mass densities instead of mass surface densities, which are used by observers, but note that these are roughly equivalent because for the most part, the stars, H I and H<sub>2</sub> are generally confined to thin disks within galaxies.

### 3.1. The Restricted Closed Box Model

In the closed box model, we consider only stars and H<sub>2</sub>, and allow  $\rho_{H_2}$  to be converted into stars at the star formation rate density, SFRD. The model is defined by Eq. 1 and

$$\frac{d\rho_{H_2}}{dt} = -SFRD. \quad (2)$$

We will for the moment consider the star formation rate, SFRD ( $= d\rho_*/dt$ ), and the gas consumption rate,  $d\rho_{H_2}/dt = -MGDR \times \rho_{H_2}$ , separately since we have observations of each individually. By comparing the observed rates as well as their time derivatives, we can test the ability of the restricted closed box model to fit observations.

We first compare  $|d\rho_{H_2}/dt|$  to the measured SFRD ( $= d\rho_*/dt$ ) today. Combining the range of  $\rho_{H_2}$  values from Obreschkow & Rawlings (2009) with the MGDR measured by Leroy et al. (2008), one obtains  $|d\rho_{H_2}/dt(z=0)| = MGDR(0) \times \rho_{H_2}(0) \sim (0.7 - 1.0) \times 10^{-2} M_\odot \text{Mpc}^{-3} \text{yr}^{-1}$ . This range of values agrees with the observed rate at which stars are forming,  $SFRD(0) \sim (0.8 - 1.8) \times 10^{-2} M_\odot \text{Mpc}^{-3} \text{yr}^{-1}$  (see §2.1) to within the uncertainties. Given that stars must form from molecular gas, this result is not surprising. Nevertheless, the agreement is reassuring because it is based on different data sets and different methods of determining the relevant quantities. It also suggests, combined with the arguments in §1 that Eq. 1 can be extrapolated to all  $z$ .

Now let us compare the time derivatives of the rates of star formation and gas consumption. First, we examine the rate of change of the molecular gas consumption. For a constant MGDR, we find  $d^2(\rho_{H_2})/dt^2 = (MGDR)^2 \rho_{H_2}$ . We showed above that at  $z=0$ ,  $SFRD = MGDR \times \rho_{H_2}$ , so at  $z=0$ , we can write  $d^2(\rho_{H_2})/dt^2 = MGDR \times SFRD \sim (.53 \text{Gyr}^{-1}) \times SFRD$ .

Now we compare this to the rate of change of the observed star formation.  $d(SFRD)/dt$  can be determined directly from the observations shown in Fig. 1. From our piecewise linear fit to the SFRD (Appendix A), we find  $d(SFRD)/dt \sim (.24 \text{Gyr}^{-1}) \times SFRD$ .

In other words, from the assumption of a constant MGDR at the present epoch in a closed box H<sub>2</sub> model, we find that the star formation rate is declining by only one half the rate at which molecular gas is being turned into stars! Is it a coincidence that the star formation rate at the present epoch is equal to the rate at which molecular gas is being converted into stars but is unequal, by large factors, at all other times? This seems highly unlikely. It is this discrepancy in the second derivatives of the stellar density and the density of H<sub>2</sub> that we call the molecular gas depletion problem. We note here that given the uncertainties in the observations, this factor of two is not a strong illustration of the molecular gas depletion problem, but we will show in the general closed box model (§3.2) that observational constraints rule out *any* closed box model.

### 3.2. The General Closed Box Model

We now relax the assumption of a constant MGDR in the closed box model in §3.1. To study the predictions of this model, we calculate  $\rho_{H_2}(z)$  by integrating Eq. (2) and using the observed SFRD( $z$ ) as an input. We then divide SFRD( $z$ ) by  $\rho_{H_2}(z)$  to obtain MGDR( $z$ ). The results are shown in Fig. 3, where  $\rho_{H_2}(0)$  is set to the mean value from Obreschkow & Rawlings (2009). The uncertainties in the SFRD (due to the IMF) discussed in §2.1 are seen to have only a minor effect on the resulting  $\rho_{H_2}(z)$  and MGDR( $z$ ).

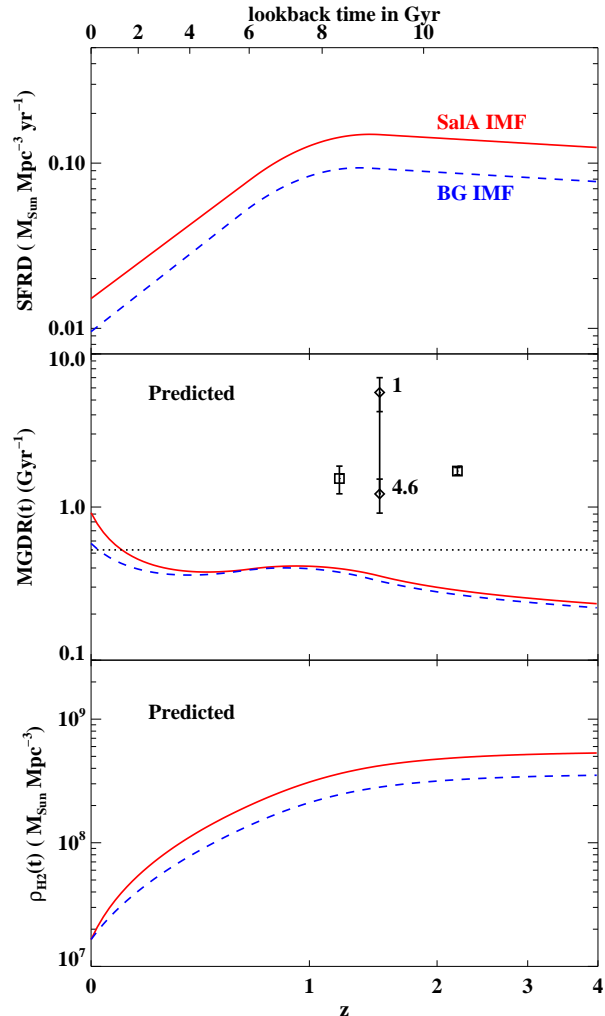


FIG. 3.— The predicted MGDR( $t$ ) and  $\rho_{H_2}(t)$  in the closed box model. The top panel shows the input SFRD forms (the smoothed piecewise linear fits from Fig. 1). The middle and bottom panels show the MGDR and  $\rho_{H_2}(t)$ , respectively, predicted by the general closed box model for these observed SFRD( $t$ ) forms. The points in the middle panel show the MGDR observations from Daddi et al. (2008) (diamonds) and from Tacconi et al. (2009) (squares), discussed in §2.2. This model requires a lower MGDR in the past, contrary to observations.

Fig. 3 shows that the solutions for  $\rho_{H_2}(t)$  increase by a factor of  $\sim 10$  from  $z=0$  to 1, and MGDR decreases with increasing redshift, contrary to the observational results discussed in §2.2. Thus, even the general closed box model is at odds with the observations, leading us

to our next model.

### 3.3. The Open Box Model

Since a closed box model of only  $H_2$  and stars is inconsistent with observations, we now allow additional components that can be converted into  $H_2$  and then into stars. We consider separately the H I gas and an external source of gas that we call  $\rho_{ext}$ , and modify Eq. (2) to

$$\frac{d\rho_{H_2}}{dt} = -SFRD - \frac{d\rho_{HI}}{dt} - \frac{d\rho_{ext}}{dt}. \quad (3)$$

#### 3.3.1. $\rho_{HI}$

For the H I gas, the observations discussed in §2.4 and Fig. 2 suggest that  $\rho_{HI}(z)$  is very slowly varying over cosmic timescales; therefore  $d\rho_{HI}/dt$  is small. Fig. 4 shows that the derivative of the observed  $\rho_{HI}$  (red curve) is an order of magnitude smaller than the observed SFRD (black curves). In the absence of  $\rho_{ext}$ , we have  $|d\rho_{H_2}/dt|$  (blue curves) is approximately equal to  $SFRD$ , as in the failed closed box model. Thus the inclusion of H I *alone* in an open-box model is not enough to fit the model to the observations. This leads to a robust conclusion: *the reservoirs of H I and  $H_2$  at all times in the past (at least as far back as  $z = 4$ ) are insufficient to fuel the star formation over cosmic timescales.*

It is important at this point to clarify that  $\rho_{HI}$  represents the reservoir of H I both in galaxies as well as the H I outside of galaxies. This is because the DLA observations of Prochaska and Wolfe (2009) include all of the high column density neutral H I ( $N(HI) > 2 \times 10^{20}$  2). This gas contains at least 85% of the neutral H I atoms for  $z < 6$  (O’Meara et al 2007).

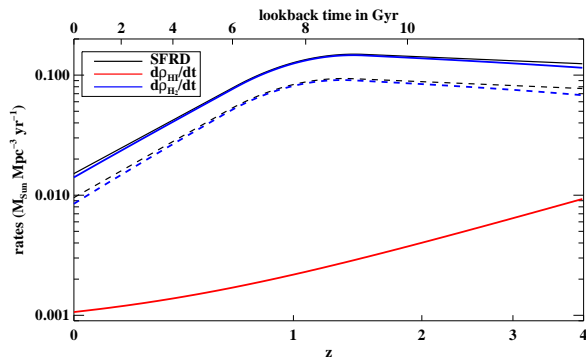


FIG. 4.— Rates of gas flowing from one phase to another in an open box model with only stars,  $H_2$  and HI (ignoring  $\rho_{ext}$ ). The SFRD (black curves) is an order of magnitude higher than  $d\rho_{HI}/dt$  (red curve), forcing  $d\rho_{H_2}/dt$  (blue curves) to be approximately equal to the SFRD, as in the closed box model. The two forms of the SFRD described in §2.1 are used: modified Sal A IMF (solid) and the Baldry & Glazebrook (2003) IMF (dashed). The derivatives of  $\rho_{HI}$  and  $\rho_{H_2}$  are negative, but the absolute values are plotted here.

#### 3.3.2. $\rho_{ext}$

We are therefore forced to include a nonzero  $d\rho_{ext}/dt$  term in the open box model. This component represents the ionized intergalactic gas at all temperatures and densities that can recombine to form H I within a Hubble

time. Effectively, it is the ionized gas in the filaments of the cosmic web.

Note that some of the H I can become ionized and redistributed to the intergalactic medium at high enough temperatures and low densities such that this gas does not recombine in a Hubble time. Such gas can be ejected by means of supernovae, galactic winds or AGN. However, if we define  $d\rho_{ext}/dt$  to be the *net* flow out of the ionized phase, then the gas that is fed back into the ionized state is implicitly included in our accounting. That is, any H I fed back into the ionized phase is made up by an equivalent increase in  $d\rho_{ext}/dt$ . If the total amount of ionized gas available is represented by  $\Omega_{baryon}$  minus the total amount of baryons in galaxies, we may consider the ionized phase to be a nearly infinite reservoir of gas available to fuel star formation. Any gas ionized and added to that reservoir by star-formation and active galaxies is negligible.

To compute the  $d\rho_{ext}/dt(t)$  required in the open box model to match the observations in §2, we start with an observed SFRD( $t$ ) and  $\rho_{HI}(t)$ , and a guess for the form of the MGDR( $t$ ) that is compatible with the limited data points from Tacconi et al. (2009) and Daddi et al. (2008). From these inputs, we compute  $\rho_{H_2}(t)$  and its time derivative using  $\rho_{H_2}(t) = SFRD(t)/MGDR(t)$ . Combining  $d\rho_{H_2}/dt$  with the observed SFRD( $t$ ) and  $d\rho_{HI}(t)/dt$  in Eq. (3) then gives  $d\rho_{ext}/dt$ . The results of this procedure are shown in Fig. 5.

To illustrate the expected range of possible values, we use two forms for the input MGDR (top panel) and two forms for the input SFRD (black dashed curves in the middle panel). For MGDR, we bracket the possible values on one side as constant using the measured value at  $z = 0$ , and on the other as one that increases linearly to larger redshifts as suggested by the Tacconi et al. (2009) and Daddi et al. (2008) data points. For the SFRD, we use the smoothed piecewise fits from Hopkins & Beacom (2006) for the two extreme IMF’s discussed in §2.1. We then calculate  $d\rho_{H_2}/dt$ ,  $d\rho_{ext}/dt$  and  $\rho_{H_2}$  for each of the four possible combinations of MGDR and SFRD. The range of calculated values is illustrated by plotting the minimum and maximum of the four curves for each calculated quantity.

In the middle panel, we note that the minimum  $\rho_{H_2}$  curve lies below  $\rho_{HI}$  at all times, and the maximum curve becomes larger than  $\rho_{HI}$  at  $z \sim 0.35$ . The difference between the two curves is mostly the MGDR choice: the maximum curve corresponds to the higher SFRD and the flat MGDR, while the minimum curve corresponds to the lower SFRD and the increasing MGDR (as expected from Eq. 1). All other combinations of MGDR and SFRD would lie between these two curves. *Because all of the molecular gas resides in galaxies, we require that the molecular gas mass in galaxies is larger, on average, at  $z = 1-2$ , than is typical at  $z = 0$ .* The change in  $\rho_{H_2}$  resulting from changing the SFRD is minor. Therefore, observations of  $\rho_{H_2}$  at  $z > 0$  or the redshift at which  $\rho_{H_2} = \rho_{HI}$  will constrain the form of the MGDR.

In the bottom panel, the absolute value of the rates is plotted, with a thicker line style used to indicate negative rates. The negative portions of the  $d\rho_{H_2}/dt$  curves correspond to decreasing  $\rho_{H_2}$  as we move forward in time towards  $z = 0$ , as  $H_2$  is converted into stars. The  $d\rho_{ext}/dt$  curves are negative for the whole range of redshifts plot-

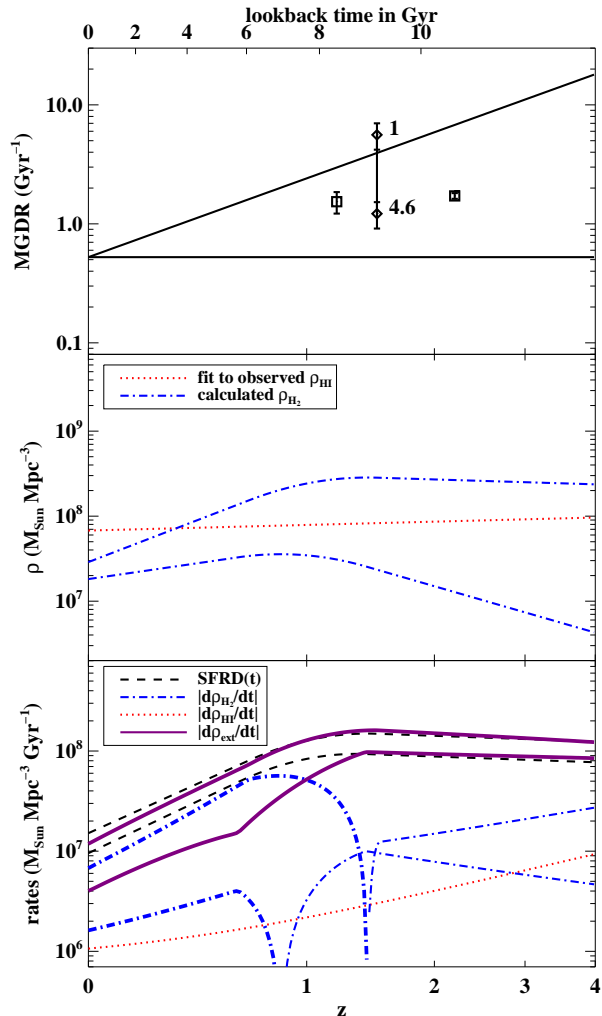


FIG. 5.— Predictions of the open box model, calculated from combinations of the inputs: two forms of the MGDR (top panel), two forms of the SFRD (middle panel) and the fit to the observations of  $\rho_{HI}$  (bottom panel). In the top panel, we plot the Tacconi et al. (2009) points (squares) as well as the Daddi et al. (2008) MGDR points for two values of  $X_{CO}$  (diamonds) to constrain the guessed range of MGDR forms. The possible range of each of the calculated quantities,  $d\rho_{H_2}/dt$ ,  $d\rho_{ext}/dt$  and  $\rho_{H_2}$ , is shown by two lines illustrating the minimum and maximum curves from the four combinations of inputs. In the bottom panel, the absolute values of the rates are plotted: thicker lines indicate negative values.

ted, indicating a flow of external gas into the H I reservoir of galaxies. We note that the range of solutions for  $d\rho_{ext}/dt$  does not deviate very much from the SFRD: roughly a factor of two at low redshifts for the minimum case. This is because the reservoirs of  $H_2$  and H I are so small compared to what is required by the observed SFRD. *Therefore, we conclude that the amount of inflow needed from this external gas,  $d\rho_{ext}/dt$ , is approximately equal to the SFRD.*

#### 4. DISCUSSION

We have shown in §3.1 and §3.2 why the closed  $H_2$  box model doesn't work. Here we discuss the constraints that can be placed on the open box model of §3.3 and what this model predicts.

##### 4.1. Variations in the SFRD

For the models in §3, we have used the SFRD prescription from Leroy et al. (2008), which finds  $SFRD \propto \rho_{H_2}$ . Some studies of galaxies with higher gas surface densities have found evidence for a steeper power law of  $SFRD \propto \rho_{H_2}^{1.4}$  (Kennicutt 1998; Wong & Blitz 2002; Bouché et al. 2007). The choice of SFRD prescription at a given redshift depends on what type of galaxies dominate the SFRD at that redshift. At the present epoch, regular spiral galaxies, such as those studied by Leroy et al. (2008), seem to dominate the SFRD: Salim et al. (2007) finds that galaxies in the mass range  $10^{9.3} < M_* < 10^{10.6} M_\odot$  account for about half of the total SFRD. At higher redshifts, however, the BzK and BX/BM galaxies dominate the SFRD (Reddy et al. 2005). These galaxies are more gas rich, and thus the  $\rho_{H_2}^{1.4}$  prescription may be more appropriate.

For this paper, we have assumed the Leroy et al. (2008) prescription for the SFRD, but note that the power law may change at higher redshift because the dominant mode of star formation may change. This is equivalent to a change in the MGDR with time, a case we consider explicitly and probably contributes to the values of the MGDR found by Tacconi et al. (2009) and Daddi et al. (2008) points. If, for example,  $SFRD = MGDR(0)\rho_{H_2}^{1.4}$  at higher redshift, then we would find  $MGDR(z) = MGDR(0)\rho_{H_2}^{0.4}$  by forcing our prescription of  $SFRD = MGDR \times \rho_{H_2}$ . Thus as  $\rho_{H_2}$  increases at higher redshift, an increase in the power law of the SFRD prescription will be manifested as an increase in the MGDR. An increase would tend to bring the MGDR closer to the upper bound in the top panel of Fig. 5, with the result that  $\rho_{H_2}(z)$  would lie closer to the lower blue curve in the bottom panel in Fig. 5.

##### 4.2. Behavior of $\rho_{H_2}(z)$

Although the exact shape of  $\rho_{H_2}$  depends sensitively on the form of MGDR, we have bounded the behavior of  $\rho_{H_2}$  by calculating what we take to be limiting cases in our open box model (Fig. 5). The  $\rho_{H_2}$  curves all rise with increasing redshift, peaking around  $z \sim 1-1.5$  at 1.5 to 10 times the value of  $\rho_{H_2}$  today. After the peak,  $\rho_{H_2}$  may fall off toward higher redshift if the MGDR is rather constant, or stay close to constant if the MGDR remains high. The prediction is less well constrained at higher redshifts. It is noteworthy that Tacconi et al. (2009) find that the gas disks they observe at  $z = 1$  and  $z = 2$  have considerably more molecular gas relative to the stars, typically about 20%, compared to  $\sim 1-5\%$  for the Milky Way and nearby disk galaxies (Helfer et al. 2003). This trend is consistent with our estimates. Although there is some uncertainty in the  $H_2$  masses of Tacconi et al. (2009) because of the uncertainty in the value of  $X_{CO}$ , there appears to be little doubt that the ratio of  $H_2$  to stellar mass in the BzK and BX/BM galaxies is higher than typical values for similar galaxies at  $z = 0$ . Due to the sensitivity of  $\rho_{H_2}$  to the form of MGDR, future observations of  $\rho_{H_2}$  or the ratio  $\rho_{H_2}/\rho_{HI}$  at higher redshift would allow us to constrain the evolution of MGDR better, and reduce the area between the bounding curves of Fig. 5.

#### 4.3. The Nature of $d\rho_{ext}/dt$

In our open box model, the H I reservoir,  $\rho_{HI}$ , is augmented by an inflow of gas from  $\rho_{ext}$  at a rate of  $10^7 - 10^8 M_\odot \text{Mpc}^{-3} \text{Gyr}^{-1}$ , depending on  $z$ . This high rate of inflow means that the gas being accreted is mostly ionized since the fraction of neutral hydrogen outside of the  $\rho_{HI}$  reservoir is too small.

The  $\rho_{HI}$  inferred from observations of DLA systems accounts for the H I associated with galactic disks. As mentioned in §3.3, O’Meara et al. (2007) find that systems with column density  $\Sigma_{HI} < 2 \times 10^{20} \text{cm}^{-2}$  account for < 15% of hydrogen atoms at all  $z < 6$ , and less than half of that is neutral. Therefore, the fraction of H I outside DLA systems is less than 7%, corresponding to roughly  $7 \times 10^6 M_\odot \text{Mpc}^{-3}$ . For an average inflow rate of a few times  $10^7 M_\odot \text{Mpc}^{-3} \text{Gyr}^{-1}$  for the past 10 Gyr, this intergalactic H I could only account for a few percent of the total, at most. Therefore, the inflow of gas needed for fueling ongoing star formation represented by  $d\rho_{ext}/dt$  must be almost completely ionized.

Recently, Dekel & Birnboim (2006) have suggested that cold flows are an important source of gas for galaxy formation and evolution. In these models, galactic disks in halos with  $M \lesssim 10^{12} M_\odot$  are built up by direct accretion of cold gaseous streams from the cosmic web. For galaxies with larger masses, cold flows are also the dominant means of mass accretion, but different outcomes for individual galaxies depend on the epoch of inflow. If this picture is correct, our work implies that the cold flows must be almost entirely ionized.

The same is true if the gas needed to fuel star formation is brought in primarily through minor mergers. If this gas were in atomic form, it would be part of the inventory of atomic gas observed in the DLA systems, which we have shown in §3.3 to contribute negligibly to fueling the star formation at all redshifts up to  $z = 4$ .

#### 4.4. Cooling Times

The open box model requires  $d\rho_{ext}/dt \sim SFRD$ , or about  $10^7$  to  $10^8 M_\odot \text{Mpc}^{-3} \text{Gyr}^{-1}$ . We use these numbers for  $d\rho_{ext}/dt$  to calculate a cooling time for the gas in the context of two models for gas accretion onto galaxies: two-phase cooling of hot halo gas (Maller & Bullock 2004) and cold flow accretion (Kereš & Hernquist 2009).

We estimate the cooling time by taking

$$\frac{\rho_{gas}}{t_{cool}} \sim \dot{\rho}_{ext}, \quad (4)$$

where  $\rho_{gas}$  is the average mass density of the cooling ionized gas smoothed over the appropriate volume (to be specified for each cooling model individually). We set  $\rho_{gas}$  equal to  $m_H n_e f$  where  $n_e$  is the local number density of electrons and  $f$  is the filling factor for the relevant volumes ( $\bar{n}_e/n_e$ ). Combining this with the cooling time

$$t_{cool} \sim \frac{3kT}{2\Lambda(T)n_e}, \quad (5)$$

gives

$$fn_e^2 \sim \frac{3kT\dot{\rho}_{ext}}{2\Lambda(T)m_H}. \quad (6)$$

As a basis for comparison, we first estimate the filling factor  $f$  for hot halos of  $L_*$  galaxies out to the

virial radius. We make the simplistic assumption that the universe is made up of  $L_*$  galaxies with masses  $M_{dyn} \sim 10^{12} M_\odot$  and circular velocities of  $\sim 160 \text{km s}^{-1}$ . Therefore, the virial radius,  $R_{vir} = GM_{dyn}/v^2 \sim 300 \text{kpc}$ . We take an average number density of  $L_*$  galaxies from Fukugita & Peebles (2004),  $n \sim .017h^3 \text{Mpc}^{-3} \sim 5.8 \times 10^{-3} \text{Mpc}^{-3}$ , and find

$$f \sim n_{L_*} \frac{4}{3} \pi R_{vir}^3 \sim 7 \times 10^{-4}. \quad (7)$$

Maller & Bullock (2004) consider gas within the cooling radius of a halo,  $R_c$ , cooling via cloud fragmentation. This results in the formation of warm ( $\sim 10^4 \text{K}$ ) clouds within the hot gas halo. In this model for the two-phase cooling of the hot halo gas, the relevant temperature for the gas is the virial temperature of the halo,  $\sim 10^6 \text{K}$  for a Milky Way type halo.

Kereš & Hernquist (2009) find that the majority of cold clouds that form around Milky Way type galaxies are the result of filamentary ”cold mode” accretion. Most of the gas does not reach the virial temperature of the halo,  $\sim 10^6 \text{K}$ , but rather cools from a maximum temperature of  $\sim 10^4 - 10^5 \text{K}$ .

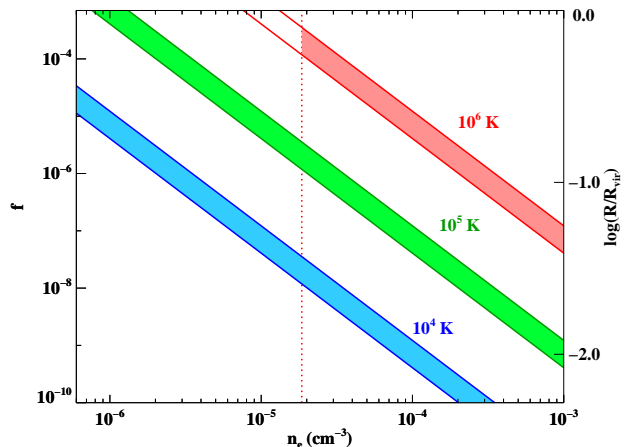


FIG. 6.— Shaded regions show the allowed filling fraction  $f$  and  $n_e$  for three temperatures:  $10^4 \text{K}$  in blue,  $10^5 \text{K}$  in green and  $10^6 \text{K}$  in red. The axis on the right gives the radius of the relevant volumes as a fraction of the virial radius corresponding to the filling fraction  $f$  in a simple universe filled with  $L_*$  galaxies. At each temperature, the allowed region of  $n_e$  vs  $f$  space is calculated using the predicted range for the inflow rate at  $z = 0$ :  $d\rho_{ext}/dt = 0.4 - 1.2 \times 10^7 M_\odot \text{Mpc}^{-3} \text{Gyr}^{-1}$ . The region is further bounded by the vertical dotted line at the value of  $n_e$  corresponding to a cooling time equal to the age of the universe. This line is only plotted for the  $10^6 \text{K}$  gas: for the other two temperatures, the densities are very small and lie outside of the plotting range.

We examine the possible values for  $n_e$  and  $f$  in these two models by calculating  $f$  as a function of  $n_e$  for three temperatures:  $10^4 \text{K}$  and  $10^5 \text{K}$  for cold flow accretion and  $10^6 \text{K}$  for cooling from the hot halo. In Fig. 6, we plot  $f$  versus  $n_e$  for these three temperatures for the range of  $d\rho_{ext}/dt$  at  $z = 0$  predicted by our open box model:  $0.4 - 1.2 \times 10^7 M_\odot \text{Mpc}^{-3} \text{Gyr}^{-1}$ . The y-axis on the right side shows  $\log(R/R_{virial})$  corresponding to  $f$ . The vertical dotted line indicates the value of  $n_e$  at which the cooling time is equal to the age of the universe. We use the approximate form for  $\Lambda(T)$  for mildly enriched gas

( $Z = 0.1$ ) from Maller & Bullock (2004) :

$$\Lambda(T) \simeq 2.6 \times 10^{-23} \left( \frac{T}{10^6 \text{ K}} \right)^{-1} \text{ cm}^{-3} \text{ erg s}^{-1} \quad (8)$$

For the cold flow gas at  $10^4$  K and  $10^5$  K, the dotted lines where the cooling times equal the age of the universe are outside of the plotting range, so the minimum allowed value of  $n_e$  is where  $R \sim R_{\text{virial}}$ : about  $8 \times 10^{-7} \text{ cm}^{-3}$  for the  $10^5$  K gas and even smaller for the  $10^4$  K gas. For the cooling hot halo gas at  $10^6$  K, the condition that the cooling time be less than the age of the universe forces  $n_e$  to be larger than about  $2 \times 10^{-5} \text{ cm}^{-3}$ .

#### 4.5. Comparing $d\rho_{\text{ext}}/dt$ to Dark Matter Accretion Rate

The rate  $d\rho_{\text{ext}}/dt$  inferred from our open box model provides an estimate for the average rate at which the baryonic fuel is required to make their way to a galactic disk in order to sustain the observed star formation, which largely occurs in the disk. A comparison of this rate with the mean rate of baryon accretion at the virial radius of the host dark matter halo will provide an estimate for the efficiency of converting the cosmological infalling baryons into stars. Many cooling and feedback processes obviously affect the fate of baryons after their infall onto the halo and whether they will reach the disk. In fact, much of the current research in galaxy formation modeling is aimed at understanding this transition. Our goal here is to estimate an overall ratio, as a function of redshift, of the baryon accretion rates at the virial radius and at the disk scale.

We begin with the dark matter accretion rate from McBride et al. (2009), which has quantified the mass accretion histories of  $\sim 500,000$  dark matter halos with masses above  $\sim 10^{12} M_{\odot}$  in the Millennium simulation of a  $\Lambda$ CDM universe (Springel et al. 2005). An approximate function is provided for the average mass accretion rate as a function of redshift and halo mass:

$$\dot{M} = \beta M_{\odot} \text{ yr}^{-1} \left( \frac{M}{10^{12} M_{\odot}} \right)^{1.127} \times (1 + 1.17z) \sqrt{\Omega_m (1+z)^3 + \Omega_{\Lambda}}. \quad (9)$$

where  $\beta \approx 42$  for the mean and  $\approx 24$  for the median rate,  $\Omega_m$  and  $\Omega_{\Lambda}$  are the present-day density parameters in matter and the cosmological constant, and  $\Omega_m + \Omega_{\Lambda}$  is assumed to be unity (as in the Millennium simulation). This  $\dot{M}$  represents the average rate at which the mass in dark matter is being accreted through the virial radius of a halo. The mass growth comes in two forms in cosmological simulations: via mergers with other resolved halos (Fakhouri & Ma 2009a), and via "diffuse" accretion of non-halo material that is a combination of unresolved halos and unbound dark matter particles (Fakhouri & Ma 2009b).

We convert  $\dot{M}$  above into a mean accretion rate for the baryons,  $\dot{M}_b$ , by assuming a cosmic baryon-to-dark matter ratio of  $f_b = \Omega_b/\Omega_m \approx 1/6$ . The result should provide a reasonable approximation for the mean rate of baryon mass that is entering the virial radius via mergers plus accretion of intergalactic gas. These infalling baryons are presumably in a mixture of forms: warm-hot ionized hydrogen gas of  $10^5$  to  $10^7$  K, "cold" flows of

$\sim 10^4$  K (still ionized) gas, and H I and stars brought in from merging galaxies. As discussed earlier, the majority of these baryons are must be in the form of H II gas.

To compare  $\dot{M}_b$  with the rate  $\dot{\rho}_{\text{ext}}$  that we calculated in §3.3 for the amount of external gas needed to account for the evolution of the observed star formation rates, we define

$$\alpha = \frac{d\rho_{\text{ext}}/dt}{f_b \dot{M} (dn/dM)}, \quad (10)$$

where  $M$  is the mass of the dark matter halo under consideration,  $\dot{M}$  is calculated using Eq. (9), and  $dn/dM$  is the (comoving) number density of dark matter halos with mass in the range of  $M$  and  $M + dM$ . The parameter  $\alpha$  represents the fraction of accreting baryons (at the virial radius) that must be converted into stars in our open box models.

The value of  $\alpha$  can be calculated by combining the allowed range of  $d\rho_{\text{ext}}/dt$  from Fig. 5 with the halo abundance  $dn/dM$  from the Millennium simulation (Springel et al. 2005). Taking  $f_b = 1/6$  and  $M = 10^{12} M_{\odot}$ , we find the predicted  $\alpha$  to be  $\sim 70 - 100\%$  at  $z \gtrsim 3$ ,  $\sim 120 - 200\%$  at  $z \sim 2$ , and  $\sim 30 - 90\%$  at  $z = 0$ . We note here that several factors may contribute to the uncertainty in the alpha values. First, alpha depends on the halo mass appropriate for the population of galaxies that dominates the SFRD at a given redshift. Using a clustering analysis, Adelberger et al. (2005) find that BzK and BX/BM galaxies ( $z \sim 2$ ) have halo masses of about  $10^{12} M_{\odot}$ , but the average value appropriate to our analysis may vary. However, since  $\dot{M} \propto M^{1.127}$  and  $M dn/dM \propto M^{-1}$  (roughly), the mass dependence is weak, so alpha changes by a maximum of  $\sim 20\%$  if we change the halo mass by a factor of 3. Second, since the  $d\rho_{\text{ext}}/dt$  calculated in our open box model roughly traces the SFRD, the alpha values, especially around  $z \sim 1 - 2$ , will be affected by the exact form of the SFRD. Finally, the large alpha value at  $z \sim 2$  may be reflecting a change in the fraction of baryons in the filaments at that redshift. Considering all the uncertainties, we make the conservative suggestion that *the open box model requires a large fraction ( $\sim 30 - 90\%$ ) of the infalling baryons at the virial radius to be turned into stars from  $z \sim 0 - 4$ .*

Another way to estimate  $\alpha$  is to compare the various  $\dot{M}$  directly. At  $z \sim 0$ , the mean baryon accretion rate from McBride et al. (2009) is  $\dot{M}_b \sim 7 M_{\odot} \text{ yr}^{-1}$  for  $10^{12} M_{\odot}$  halos, and the measured star formation rate in the Milky Way ranges from  $\dot{M}_* \sim 2 M_{\odot} \text{ yr}^{-1}$  to  $\sim 4 M_{\odot} \text{ yr}^{-1}$  (Miller & Scalo (1979); Diehl et al. (2006)). These rates imply  $\alpha \sim \dot{M}_*/\dot{M}_b \sim 20$  to  $60\%$ . In addition, we can use the predicted  $\dot{\rho}_{\text{ext}}$  from our open box models to estimate a mean conversion rate of external H II gas into stars per galaxy,  $\dot{M} \sim \dot{\rho}_{\text{ext}}/n_{L_*}$ . Taking  $\dot{\rho}_{\text{ext}} \sim 10^7 M_{\odot} \text{ Mpc}^{-3} \text{ Gyr}^{-1}$  from Fig. 5 and  $n_{L_*} \sim 6 \times 10^{-3} \text{ Mpc}^{-3}$  for the number density of  $L_*$  galaxies today, we obtain a rate of  $\sim 2 M_{\odot} \text{ yr}^{-1}$ , which is consistent with the star formation rate in the Milky Way.

## 5. SUMMARY AND CONCLUSIONS

We have used the observed Star Formation Rate Density (SFRD), Molecular Gas Depletion Rate (MGDR), and volume averaged density of molecular hydrogen

( $\rho_{H_2}$ ) and atomic hydrogen ( $\rho_{HI}$ ) to determine the mass flow rates and densities of the star-forming gas back to  $z \simeq 4$ . Extrapolations further back in time are primarily limited by uncertainties in the SFRD. We find that:

- There are no models of gas consumption where the reservoir of gas is either only  $H_2$  or both  $H\ I$  and  $H_2$ , that are compatible with the observations of molecular gas in the galaxies at  $z \sim 2$  that produce the observed SFRD.
- Inflowing ionized intergalactic gas must provide most of the gas that turns into stars to times as early as  $z \sim 4$ . There is so little neutral gas inflow at all epochs, that the neutral gas ought to be considered more as a phase of cosmic gas flow than a reservoir of star forming gas.
- From  $z \simeq 1 - 4$ , the rate of mass inflow from the ionized state to the atomic state is  $1 - 2 \times 10^8 M_\odot \text{Mpc}^{-3} \text{Gy}^{-1}$ . At  $z \lesssim 1$ , the mass flow rate varies linearly from about  $0.5 \times 10^7 M_\odot \text{Mpc}^{-3} \text{Gy}^{-1}$  at  $z = 0$  to about  $1.5 \times 10^8 M_\odot \text{Mpc}^{-3} \text{Gy}^{-1}$ . There is sufficient amount of infalling baryons at the virial radius of the halos from the cosmic web to supply

these mass inflows onto the galactic disk; at all redshifts, the mass inflow rate is at least 30% of the infalling rate.

- For all models, the volume averaged density of  $H_2$  increases from its present value by a factor of 1.5 to 10 at  $z = 1 - 2$  depending mostly on  $MGDR(t)$ .

---

This work has been partially supported by NSF grant AST-0838258. LB would also like to acknowledge Distinguished Visitor Awards from the University of Sydney and CSIRO as well as a visiting scholar award from the Center for Astrophysics, where much of the present work was done. We would like to thank Reinhard Genzel and Linda Tacconi for use of their results prior to publication, and conversations with many people including Robert Braun, Avi Loeb, Dusan Keres, Norm Murray and Eliot Quataert.

#### REFERENCES

- Adelberger, K. L., Steidel, C. C., Pettini, M., Shapley, A. E., Reddy, N. A., & Erb, D. K. 2005, *ApJ*, 619, 697
- Alves, J., Lombardi, M., & Lada, C. J. 2007, *A&A*, 462, L17
- Baldry, I. K., & Glazebrook, K. 2003, *ApJ*, 593, 258
- Blaauw, A. 1964, *ARA&A*, 2, 213
- Bouché, N., et al. 2007, *ApJ*, 671, 303
- Burton, W. B., Liszt, H. S., & Baker, P. L. 1978, *ApJ*, 219, L6
- Carilli, C. L., et al. 2002, *AJ*, 123, 1838
- Cazaux, S., & Tielens, A. G. G. M. 2004, *ApJ*, 604, 222
- Cole, S., et al. 2001, *MNRAS*, 326, 255
- Daddi, E., Dannerbauer, H., Elbaz, D., Dickinson, M., Morrison, G., Stern, D., & Ravindranath, S. 2008, *ApJ*, 673, L21
- Dekel, A., & Birnboim, Y. 2006, *MNRAS*, 368, 2
- Diehl, R. et al. 2006, *Nature*, 439, 45
- Fakhouri, O., & Ma, C.-P. 2009a, *MNRAS*, 394, 1825
- Fakhouri, O., & Ma, C.-P. 2009b, arXiv:0808.2471
- Forster Schreiber, N. M., et al. 2009, arXiv:0903.1872
- Fukugita, M., & Peebles, P. J. E. 2004, *ApJ*, 616, 643
- Gao, Y., & Solomon, P. M. 2004, *ApJ*, 606, 271
- Gil de Paz, A., et al. 2007, *ApJS*, 173, 185
- Grcevich, J., & Putman, M. E. 2009, *ApJ*, 696, 385
- Hanish, D. J., et al. 2006, *ApJ*, 649, 150
- Helfer, T. T., Thornley, M. D., Regan, M. W., Wong, T., Sheth, K., Vogel, S. N., Blitz, L., & Bock, D. C.-J. 2003, *ApJS*, 145, 259
- Herbig, G. H., & Kameswara Rao, N. 1972, *ApJ*, 174, 401
- Hippelein, H., et al. 2003, *A&A*, 402, 65
- Hollenbach, D., & Salpeter, E. E. 1971, *ApJ*, 163, 155
- Hopkins, A. M., & Beacom, J. F. 2006, *ApJ*, 651, 142
- Houck, J. R., Weedman, D. W., Le Floch, E., & Hao, L. 2007, *ApJ*, 671, 323
- Kennicutt, R. C. 1998, *ApJ*, 498, 541
- Kennicutt, R. C., Jr., et al. 2003, *PASP*, 115, 928
- Kereš, D., & Hernquist, L. 2009, arXiv:0905.2186
- Lada, E. A. 1992, *ApJ*, 393, L25
- Lah, P., et al. 2007, *MNRAS*, 376, 1357
- Leroy, A. K., Walter, F., Brinks, E., Bigiel, F., de Blok, W. J. G., Madore, B., & Thornley, M. D. 2008, *AJ*, 136, 2782
- Madau, P., Ferguson, H. C., Dickinson, M. E., Giavalisco, M., Steidel, C. C., & Fruchter, A. 1996, *MNRAS*, 283, 1388
- Maller, A. H., & Bullock, J. S. 2004, *MNRAS*, 355, 694
- McBride, J., Fakhouri, O., & Ma, C.-P. 2009, arXiv:0902.3659
- Miller, G. E., & Scalo, J. M. 1979, *ApJS*, 41, 513
- Motte, F., Andre, P., & Neri, R. 1998, *A&A*, 336, 150
- Myers, P. C. 2008, *ApJ*, 687, 340
- Obreschkow, D., & Rawlings, S. 2009, *MNRAS*, 289
- O'Meara, J. M., Prochaska, J. X., Burles, S., Prochter, G., Bernstein, R. A., & Burgess, K. M. 2007, *ApJ*, 656, 666
- Omont, A., Petitjean, P., Guilloteau, S., McMahon, R. G., Solomon, P. M., & Pécontal, E. 1996, *Nature*, 382, 428
- Prochaska, J. X., & Wolfe, A. M. 2009, *ApJ*, 696, 1543
- Rao, S. M., Turnshek, D. A., & Nestor, D. B. 2006, *ApJ*, 636, 610
- Reddy, N. A., Erb, D. K., Steidel, C. C., Shapley, A. E., Adelberger, K. L., & Pettini, M. 2005, *ApJ*, 633, 748
- Salim, S., et al. 2007, *ApJS*, 173, 267
- Schwartz, P. R., Wilson, W. J., & Epstein, E. E. 1973, *ApJ*, 186, 529
- Shu, F. H., Adams, F. C., & Lizano, S. 1987, *ARA&A*, 25, 23
- Springel, V., et al. 2005, *Nature*, 435, 629
- Steidel, C. C., Adelberger, K. L., Giavalisco, M., Dickinson, M., & Pettini, M. 1999, *ApJ*, 519, 1
- Tacconi, L., et. al. 2009, *ApJ*, submitted
- Walter, F., Brinks, E., de Blok, W. J. G., Bigiel, F., Kennicutt, R. C., Thornley, M. D., & Leroy, A. 2008, *AJ*, 136, 2563
- Wolfe, A. M., Gawiser, E., & Prochaska, J. X. 2005, *ARA&A*, 43, 861
- Wong, T., & Blitz, L. 2002, *ApJ*, 569, 157
- Zwaan, M. A., Meyer, M. J., Staveley-Smith, L., & Webster, R. L. 2005, *MNRAS*, 359, L30
- Zwaan, M. A., & Prochaska, J. X. 2006, *ApJ*, 643, 675

#### APPENDIX

##### A. FUNCTIONAL FORM FOR THE SFRD

The form for the SFRD used throughout the paper is a smoothed form of the piecewise fits from Hopkins & Beacom (2006). The original piecewise function is defined by intercept and slope  $a$  and  $b$  for  $z < z_1$  and  $c$  and  $d$  for  $z > z_1$  (we only consider  $z < 4$ ). The smoothed section is just a quadratic form in the  $\log(1+z)$  vs  $\log(SFRD)$  plane over a

distance  $2\Delta$  in  $\log(1+z)$ . We give the piecewise function for the SFRD below, with  $x = \log(1+z)$  and  $x_1 = \log(1+z_1)$ .

$$\log(SFRD) = \begin{cases} a + bx & 0 \leq x \leq x_1 - \Delta \\ a + b(x_1 - \Delta) + \frac{(d-b)}{4\Delta} (x^2 - (x_1 - \Delta)^2) & \\ + \frac{1}{2} \left[ b + d + (b-d) \frac{x_1}{\Delta} \right] (x - x_1 + \Delta) & x_1 - \Delta \leq x \leq x_1 + \Delta \\ c + dx & x_1 + \Delta \leq x \leq x_{max} \end{cases} \quad (\text{A1})$$

In the table below, we give a,b,c,d and z1 for each of the two piecewise linear fits from Hopkins & Beacom (2006) (for the Modified Salpeter A IMF and the Baldry & Glazebrook (2003) IMF). To produce reasonable smoothing, we used  $2\Delta = \log(1.5)$ .

	Mod SalA IMF	BG 2003 IMF
a	-1.82	-2.02
b	3.28	3.44
c	-0.724	-0.930
d	-0.26	-0.26
z1	1.04	0.97

TABLE 1

TABLE OF FIT PARAMETER VALUES FOR THE TWO PIECEWISE LINEAR FITS FROM HOPKINS & BEACOM (2006): THE MODIFIED SALPETER A IMF AND THE BALDRY & GLAZEBROOK (2003) IMF.